Developmental Cell
Article

Resistance to Caspase-Independent Cell Death Requires Persistence of Intact Mitochondria

Stephen W.G. Tait,[1] Melissa J. Parsons,[1] Fabien Llambi,[1] Lisa Bouchier-Hayes,[1] Samuel Connell,[2] Cristina Muñoz-Pinedo,[3] and Douglas R. Green[1,*]
[1]Department of Immunology
[2]Cell and Tissue Imaging
St. Jude Children's Research Hospital, 262 Danny Thomas Place, Memphis, TN 38105, USA
[3]Institut d'Investigació Biomèdica de Bellvitge, Barcelona, 08907, Spain
*Correspondence: douglas.green@stjude.org
DOI 10.1016/j.devcel.2010.03.014

SUMMARY

During apoptosis, mitochondrial outer membrane permeabilization (MOMP) is often a point-of-no-return; death can proceed even if caspase activation is disrupted. However, under certain conditions, resistance to MOMP-dependent, caspase-independent cell death is observed. Mitochondrial recovery represents a key process in this survival. Live cell imaging revealed that during apoptosis not all mitochondria in a cell necessarily undergo MOMP. This incomplete MOMP (iMOMP) was observed in response to various stimuli and in different cell types regardless of caspase activity. Importantly, the presence of intact mitochondria correlated with cellular recovery following MOMP, provided that caspase activity was blocked. Such intact mitochondria underwent MOMP in response to treatment of cells with the Bcl-2 antagonist ABT-737, suggesting that the resistance of these mitochondria to MOMP lies at the point of Bax or Bak activation. Thus, iMOMP provides a critical source of intact mitochondria that permits cellular survival following MOMP.

INTRODUCTION

In response to most stimuli, engagement of apoptosis involves mitochondrial outer membrane permeabilization (MOMP), which in turn leads to widespread activation of executioner caspases. The proteolytic activity of these caspases causes the physiological hallmarks of apoptosis, including DNA fragmentation, nuclear condensation, phosphatidylserine externalization, and plasma membrane blebbing (Taylor et al., 2008). Although caspase activation is the defining characteristic of apoptosis, cells that undergo MOMP but are prevented from activating executioner caspases by chemical inhibitors or by genetic ablation of Apaf-1 or caspase-9 will nonetheless die (Amarante-Mendes et al., 1998; Haraguchi et al., 2000; McCarthy et al., 1997; Xiang et al., 1996). MOMP-dependent, caspase-independent cell death (CICD) may be due to loss of mitochondrial function caused by MOMP, and/or by release of mitochondrial proteins that can kill a cell in a caspase-independent manner (Tait and Green, 2008). Examples of the latter include AIF, Omi/HtrA2 and Endonuclease G, although their roles in mediating CICD remain controversial (Li et al., 2001; Susin et al., 1999; Suzuki et al., 2001). That CICD is dependent on MOMP is evidenced by observations that expression of antiapoptotic Bcl-2 proteins (Haraguchi et al., 2000) or lack of the proapoptotic Bcl-2 effectors, Bax and Bak, (Lum et al., 2005) prevents cell death.

These findings have led to the view that MOMP represents a point-of-no-return for cell death. However, this is not always the case. For example, postmitotic sympathetic neurons deprived of neurotrophic factor undergo MOMP but remain viable provided caspase activity is inhibited and growth factor is replenished (Deshmukh et al., 2000; Martinou et al., 1999). Recently, we found that proliferating cells can also recover following MOMP. By employing a retroviral based cDNA screen for inhibitors of CICD, we identified glyceraldehyde-3-phosphate dehydrogenase (GAPDH) as being able to promote cellular survival following MOMP and allow clonogenic outgrowth (Colell et al., 2007). This protective effect of GAPDH was dependent upon its well-defined glycolytic role and a novel role in stimulating mitophagy, in part, through upregulation of Atg12.

The ability of cells to recover from MOMP has a variety of clinical implications, including implications for oncogenesis. For example, tumor cell lines often display reduced caspase activity owing to a lack of Apaf-1 expression, apoptosome activity, or caspase expression (Devarajan et al., 2002; Ferreira et al., 2001; Soengas et al., 2001; Wolf et al., 2001). Alternatively, some tumors overexpress inhibitor of apoptosis proteins (IAPs) that can directly inhibit caspase function (Krajewska et al., 2003; Tamm et al., 2000). Moreover, expression of a dominant negative form of caspase-9 in vivo (which prevents caspase activation following MOMP) has been shown to enhance survival and proliferation of transformed cells (Schmitt et al., 2002). These studies suggest that tumor cells have developed means of inhibiting caspase activity downstream of MOMP. The ability of tumor cells to recover and proliferate after MOMP would facilitate tumor cell survival and chemotherapeutic resistance.

How mitochondrial repopulation occurs during cellular recovery from MOMP is unknown. Mitochondrial function is critical for survival following MOMP because only cells that maintain $\Delta\Psi_m$ are able to survive (Colell et al., 2007; Deshmukh et al., 2000). However, in order to recover from MOMP and proliferate, cells must either generate or already possess a source of healthy, intact mitochondria. In this study we set out to address how cells, following MOMP, can produce an essential pool of intact mitochondria to enable cellular survival.

RESULTS

Incomplete Mitochondrial Outer Membrane Permeabilization during Apoptosis

To facilitate study of mitochondrial repopulation following MOMP, we first sought to define a system in which intact mitochondria could readily be distinguished from permeabilized mitochondria via single-cell imaging of live cells. Previous studies have shown that, provided caspase activity is inhibited, Smac/Diablo and Omi are degraded in a proteasome-dependent manner following their release from mitochondria during apoptosis (MacFarlane et al., 2002; Sun et al., 2004). We reasoned that Smac and Omi fluorescent fusion proteins might also be degraded following MOMP, thereby facilitating the detection of intact mitochondria, which would remain bright. To address this, we generated HeLa cells stably expressing Smac-GFP or Omi-mCherry. Both Smac-GFP and Omi-mCherry displayed appropriate mitochondrial localization and were released from mitochondria following cell treatment with the apoptotic stimulus actinomycin D (ActD) (data not shown). Next, we treated HeLa cells expressing Smac-GFP or Omi-mCherry with staurosporine (STS) in the presence of the pan-caspase inhibitor quinolyl-valyl-O-methylaspartyl-[2,6-difluorophenoxy]-methyl ketone (Q-VD-OPh) and examined them by live-cell microscopy. HeLa cells stably expressing cytochrome *c*-GFP have been previously described and were used for comparison (Goldstein et al., 2005). The total brightness of cells was assessed and plotted relative to the onset of MOMP (Figure 1A). Mitochondrial release of Smac-GFP and Omi-mCherry was rapid and occurred with similar kinetics as cytochrome *c*, consistent with previous results (Munoz-Pinedo et al., 2006). However, unlike cytochrome *c*, Smac-GFP and Omi-mCherry were degraded following MOMP, as detected by a gradual loss of fluorescence that initiated at the onset of MOMP. These results demonstrate that Smac-GFP and Omi-mCherry display appropriate mitochondrial localization, are released with the expected kinetics following MOMP, and similar to endogenous Smac and Omi, are degraded following MOMP.

We next employed these fluorescent tools to investigate if a limited number of intact mitochondria persist in cells following MOMP. HeLa cells expressing Smac-GFP were treated with ActD in the presence of Q-VD-OPh and imaged by live-cell microscopy (Figure 1B; see Movie S1 available online). Although MOMP, corresponding to rapid mitochondrial release of Smac-GFP, was readily detected in these cells, we noticed that in many cells MOMP appeared to be incomplete such that certain mitochondria failed to undergo permeabilization, as evidenced by a continued punctate distribution of Smac-GFP. We define this incomplete MOMP (iMOMP) as the persistence of a subset of intact mitochondria within a cell that has undergone MOMP. Incomplete MOMP was confined to a minority of mitochondria within the cell (Figure 1B) and was also observed in response to UV or STS treatment in the presence of Q-VD-OPh (Figure S1A). Quantification of cells that displayed iMOMP revealed that, regardless of apoptotic stimulus, approximately 25% of cells displayed iMOMP (Figure 1C). To verify that the remaining punctate Smac-GFP following MOMP was localized to mitochondria we treated HeLa cells expressing Smac-GFP and mitochondrial matrix targeted dsRed (mito dsRed) with UV and Q-VD-OPh and then imaged them by live-cell microscopy (Figure 1D). In cells that displayed iMOMP, the punctate Smac-GFP signal co-localized with the mito dsRed signal indicating that it was indeed localized to the mitochondria. Other mitochondrial intermembrane space (IMS) proteins besides Smac-GFP were also used to visualize iMOMP. HeLa cells coexpressing Smac-GFP and Omi-mCherry were treated with ActD plus Q-VD-OPh and imaged by live-cell microscopy (Figure 1E). Following treatment, in some cells, Omi-mCherry displayed punctate distribution following MOMP that colocalized with Smac-GFP. Furthermore, we also found that upon treatment of HeLa cells expressing cytochrome *c*-GFP with ActD or UV, puncta corresponding to mitochondrially localized cytochrome *c*-GFP persisted following MOMP in some cells (Figure S1B). These results demonstrate that iMOMP can be detected using a variety of IMS fluorescent fusion proteins. We further investigated whether iMOMP could be detected by examining endogenous IMS protein distribution following MOMP. HeLa cells expressing Smac-GFP were treated with UV or ActD in the presence of Q-VD-OPh, and immunostained for endogenous cytochrome *c* (Figure 1F). In untreated cells, cytochrome *c* and Smac-GFP displayed complete colocalization. Following apoptotic stimuli, continued mitochondrial colocalization of cytochrome *c* and Smac-GFP in a subset of intact mitochondria was detected in some cells undergoing MOMP, demonstrating that iMOMP can also be detected by examination of endogenous IMS proteins. In addition we examined the colocalization of endogenous Smac and cytochrome *c* with mito dsRed, and observed that in cells that had undergone MOMP following treatment with STS there was persistence of puncta corresponding to mitochondrially localized cytochrome *c* or Smac (Figure S1C). Collectively, these data demonstrate that during apoptosis MOMP can be incomplete, leaving some mitochondria intact.

Incomplete MOMP Is Cell-Type and Caspase Independent

To extend our observations to other cell lines, MCF-7 cells stably expressing Smac-GFP were generated. We then treated these cells with ActD plus Q-VD-OPh or TNF without caspase inhibitors and examined them by live-cell imaging (Figure 2A). Smac-GFP was released from the majority of mitochondria, yet punctate Smac-GFP distribution persisted in some cells. Following UV plus Q-VD-OPh treatment the punctate distribution of Smac following MOMP colocalized with matrix mCherry, demonstrating that the observed puncta corresponded to mitochondria (Figure 2B; Movie S2). We also examined the permeabilization of mitochondria in MCF-7 cells coexpressing Smac-GFP and Omi-mCherry following treatment with ActD in the presence of Q-VD-OPh and assessed by live-cell imaging (Figure 2C). Incomplete release of Omi-mCherry was observed in the same intact mitochondria that failed to release Smac-GFP, similar to our results in HeLa cells. Finally, we also treated wild-type murine embryonic fibroblasts (WT MEFs) stably expressing Omi-mCherry and examined them by live-cell microscopy. Similar to other cell types tested, iMOMP was detected in WT MEFs as evidenced by continued mitochondrial retention of Omi-mCherry following MOMP (Figure S2).

Studies have suggested that caspase activity is required to ensure complete MOMP during apoptosis (Lakhani et al.,

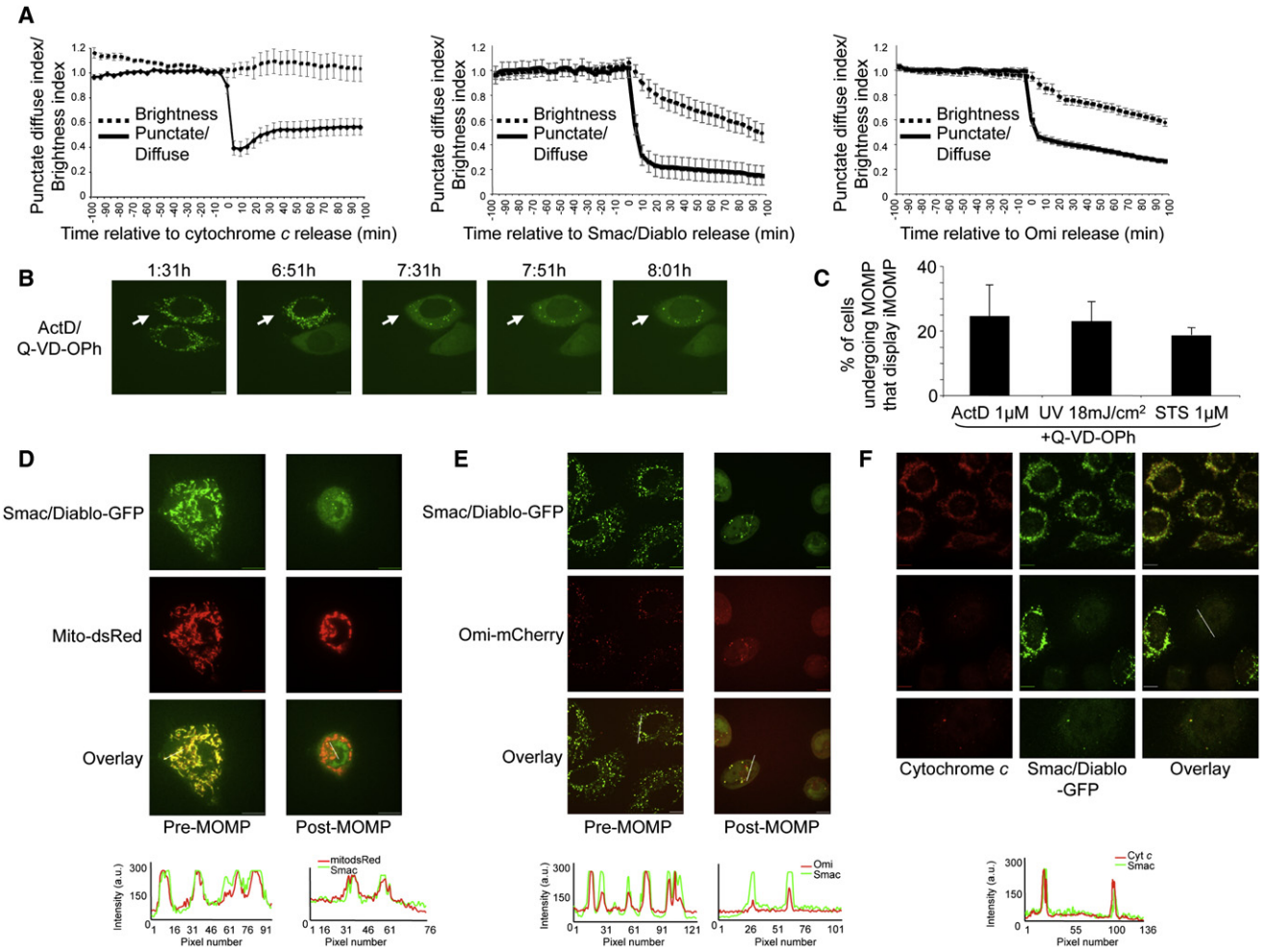

Figure 1. Incomplete Mitochondrial Outer Membrane Permeabilization during Apoptosis

(A) HeLa cells expressing Omi-mCherry, Smac-GFP, or cytochrome *c*-GFP were treated with STS (1 μM) plus Q-VD-OPh (20 μM) and imaged every 5 min. Regions were drawn around cells, and punctate/diffuse and brightness indices were plotted and displayed relative to the onset of MOMP (time point 0). Data were scaled and represent the average of 15 cells. Error bars represent standard error of the mean.

(B) HeLa cells expressing Smac-GFP were treated with STS (1 μM) or ActD (1 μM) plus Q-VD-OPh (20 μM) and imaged every 10 min by live-cell confocal microscopy. Representative confocal micrographs covering the onset and duration of MOMP are shown. The time of each frame relative to the start of image acquisition is shown. Arrows denote cells undergoing iMOMP.

(C) HeLa cells expressing Smac-GFP were treated for 16 hr with STS (1 μM), ActD (1 μM), or UV (18 mJ/cm^2) plus Q-VD-OPh (20 μM) and quantified for the occurrence of iMOMP. The percentage cells displaying iMOMP as a percentage of cells that had undergone MOMP (minimum 100 cells counted) is shown and error bars represent the standard deviation (SD) from three independent experiments.

(D) HeLa cells expressing Smac-GFP and mito-dsRed were treated with UV (18mJ/cm^2) plus Q-VD-OPh (20 μM) and imaged every 10 min by live-cell confocal microscopy. Representative confocal micrographs covering the onset and duration of MOMP are shown. Arrows denote cells undergoing iMOMP. Line scans indicate colocalization of Smac-GFP and mito-dsRed and correlate to the line drawn in the images (E) HeLa cells expressing Smac-GFP and Omi-mCherry were treated with ActD (1 μM) plus Q-VD-OPh (20 μM) and imaged every 10 min by live-cell confocal microscopy. Representative confocal micrographs pre- and post-MOMP are shown. Arrows denote cells undergoing iMOMP. Line scans indicate colocalization of Smac-GFP and Omi-mCherry and correlate to the lines drawn in the images (F) HeLa cells expressing Smac-GFP were treated for 16 hr with UV (18 mJ/cm^2) plus Q-VD-OPh (20 μM), fixed and immunostained with anti-cytochrome *c* antibody. Representative confocal micrographs pre- and post-MOMP are shown. Line scans indicate colocalization of Smac-GFP and cytochrome *c* and correlate to the line drawn in the images. Scale bars represent 10 μm. See also Figure S1.

2006). We addressed whether iMOMP was due to the inhibition of caspase activity by carrying out live-cell imaging of TNF-treated HeLa cells expressing Smac-GFP in the absence of caspase inhibitors (Figure 2D; Movie S3). Propidium iodide uptake was used to assess plasma membrane permeabilization. Incomplete MOMP was observed in the absence of caspase inhibitors, as evidenced by the presence of intact mitochondria in cells that had undergone caspase-dependent plasma membrane permeabilization. These data demonstrate that iMOMP occurs independently of caspase activity and in different cell types.

Characterization of iMOMP

We next addressed whether any intact mitochondria that remained following MOMP were functional by examining whether

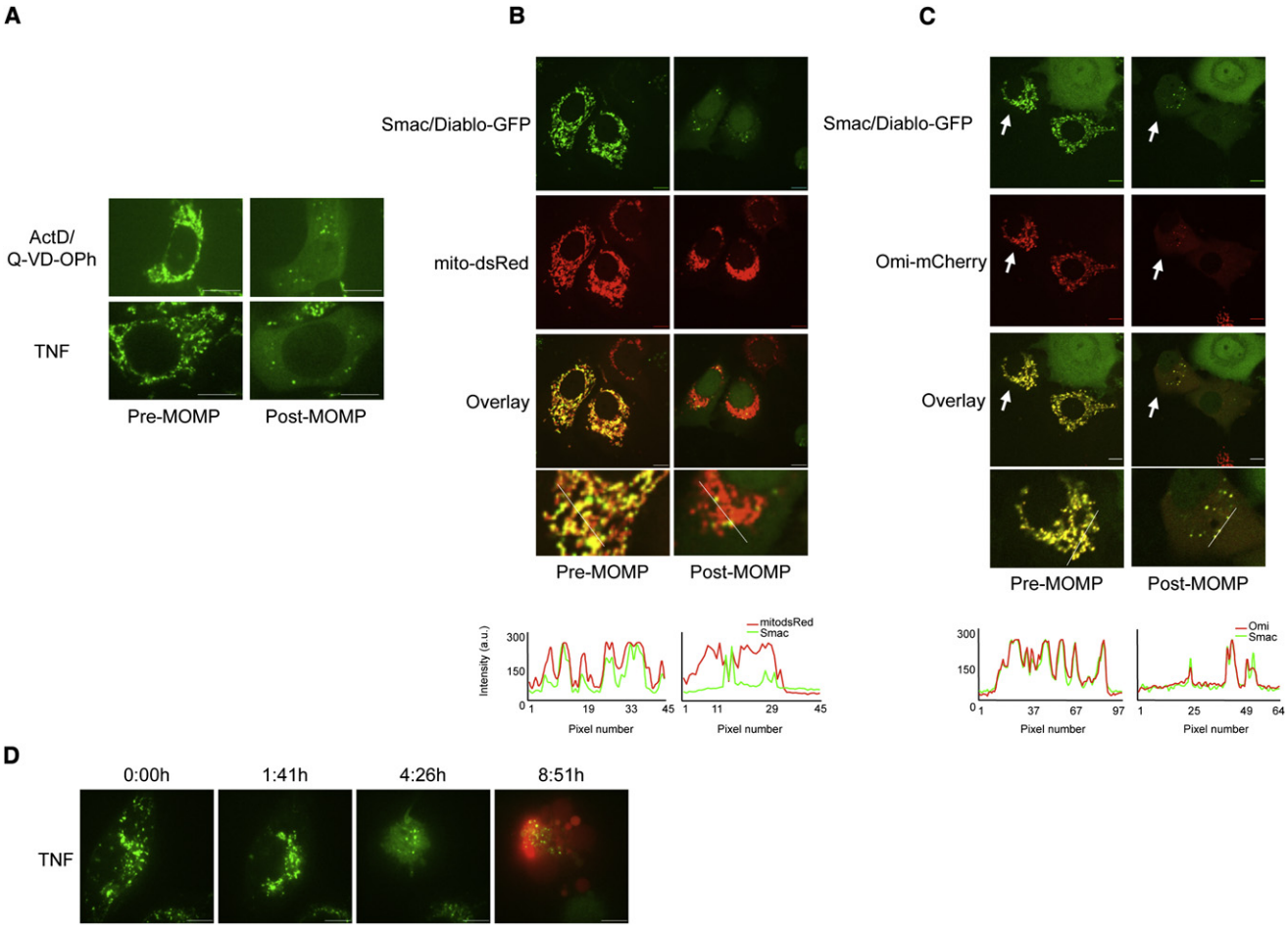

Figure 2. Incomplete MOMP Is Cell-Type and Caspase Independent

(A) MCF-7 cells expressing Smac-GFP were treated with UV (18 mJ/cm^2) plus Q-VD-OPh (20 μM) or TNF (10 ng/ml) and imaged every 10 min by live-cell confocal microscopy. Representative confocal micrographs pre- and post-MOMP are shown.

(B) MCF-7 cells expressing Smac-GFP and matrix-targeted mCherry were treated with ActD (1 μM) plus Q-VD-OPh (20 μM) and imaged every 10 min by live-cell confocal microscopy. Representative confocal micrographs pre- and post-MOMP are shown. Line scans indicate colocalization of Smac-GFP and mito-dsRed and correlate to the line drawn in the images.

(C) MCF-7 cells expressing Smac-GFP and Omi-mCherry were treated with ActD (1 μM) plus Q-VD-OPh (20 μM) and imaged every 10 min by live-cell confocal microscopy. Representative confocal micrographs pre- and post-MOMP are shown and arrows denote cells undergoing iMOMP.

(D) HeLa cells expressing Smac-GFP were treated with TNF (10 ng/ml) in the presence of propidium iodide (1 μg/ml) and imaged every 10 min by live-cell confocal microscopy. Representative confocal micrographs pre- and post-MOMP are shown. Scale bars represent 10 μm. See also Figure S2.

these mitochondria maintained $\Delta\Psi_m$. HeLa cells expressing Smac-GFP were treated with STS in the presence of Q-VD-OPh for 1 or 4 days, incubated with the potentiometric dye TMRE, and imaged (Figure 3A). In line with published data (Waterhouse et al., 2001), at 1 day post-MOMP many mitochondria maintained $\Delta\Psi_m$, as determined by TMRE positivity. At later time points (4 days), intact mitochondria maintained $\Delta\Psi_m$, as shown by colocalization of Smac-GFP and TMRE.

Protection from CICD following MOMP typically occurs over several days, involving removal of mitochondria by mitophagy and requires mitochondrial repopulation (Colell et al., 2007). Therefore, we imaged cells over extended time periods to investigate the fate of intact mitochondria. MCF-7 cells expressing Smac-GFP were treated with UV in the presence of Q-VD-OPh and followed over a period of 3 days. In cells displaying iMOMP, intact mitochondria that had failed to undergo MOMP typically persisted in cells over 3 days, indicating that failure of mitochondria to undergo MOMP is long-lived (Figure S3). Intriguingly, in some cells mitochondrial repopulation occurred following MOMP, which was visualized by a gradual increase in Smac-GFP puncta over time (Figure 3B; Movie S4). Closer examination revealed several examples of apparent division of intact mitochondria, occurring even at early time points post-MOMP (Figure 3C).

Following from these findings, we addressed the effect of mitochondrial dynamics on iMOMP. Mitochondrial fission was induced through transient addition of p-trifluoromethoxy carbonyl cyanide phenyl hydrazone (FCCP), which is known to induce mitochondrial fission by a Drp-1-dependent mechanism (Cereghetti et al., 2008). Conversely, inhibition of

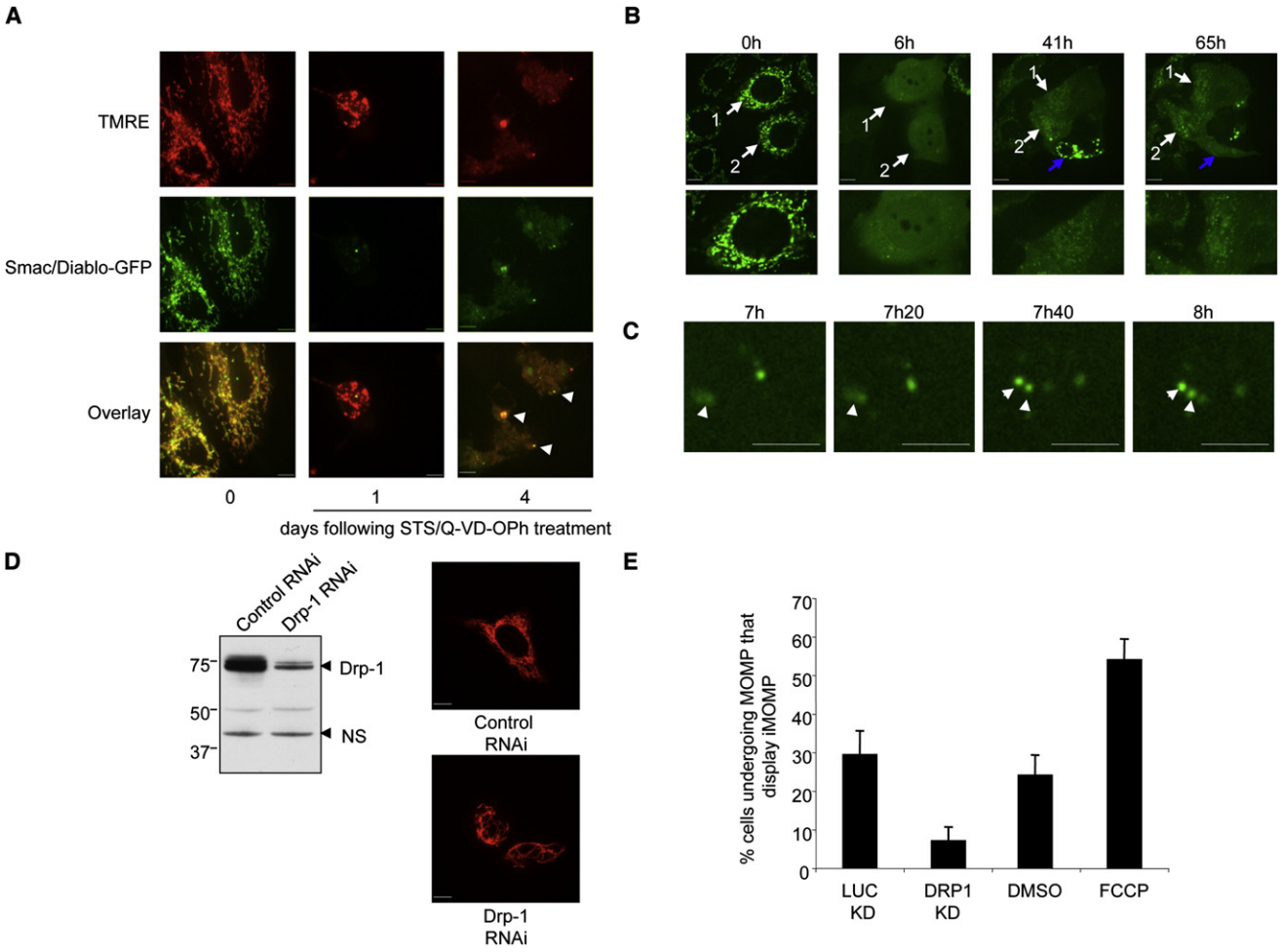

Figure 3. Characterization of iMOMP

(A) HeLa cells expressing Smac-GFP were treated with STS (1 μM) and Q-VD-OPh (20 μM). At various times posttreatment cells were incubated with TMRE (50 nM) and imaged by confocal microscopy. Representative images are shown and arrows denote intact mitochondria.

(B) MCF-7 cells expressing Smac-GFP were treated with UV (18 mJ/cm^2) plus Q-VD-OPh (20 μM) and imaged every 20 min by live-cell confocal microscopy. Numbered arrows denote the same cell at different time points. Blue arrow denotes cell that undergoes MOMP at a late time point. The time of each frame relative to the start of image acquisition is shown.

(C) Magnified panels from experiment described in (B). The time of each frame relative to the start of image acquisition is shown.

(D) Left: HeLa cells were transfected with control or Drp-1 targeting shRNA vectors. Four days posttransfection and selection, cells were probed for Drp-1 levels by western blot; ns denotes nonspecific protein used as loading control. Right: HeLa or HeLa Drp-1 knockdown cells expressing mito-dsRed were analyzed by confocal microscopy, and representative micrographs are shown.

(E) HeLa cells expressing mito-dsRed and Smac-GFP treated with DMSO or FCCP (50 μM) and Drp-1 knockdown or control cells expressing mito-dsRed and Smac-GFP were treated with STS (1 μM) and Q-VD-OPh (20 μM). Following overnight treatment, cells were assessed. Scale bars represent 10 μm. See also Figure S3.

mitochondrial fission was achieved by shRNA-mediated down-regulation of Drp-1. Efficient knockdown of Drp-1, as detected by immunoblot, resulted in cells with hyperfused mitochondrial networks (Figure 3D). HeLa expressing Smac-GFP and mito dsRed were then treated with STS in the presence of Q-VD-OPh and assessed for iMOMP the following day. Inhibition of mitochondrial fission through Drp-1 knockdown effectively reduced the incidence of iMOMP (Figure 3E). In contrast, promotion of fission by FCCP treatment increased the number of cells displaying iMOMP (Figure 3E). Taken together, these results demonstrate a role for mitochondrial dynamics in the phenomenon of iMOMP.

Incomplete MOMP Correlates with Protection from CICD

Incomplete MOMP represents a means of providing nonpermeabilized mitochondria that may facilitate cellular recovery following MOMP. To determine whether there was a direct correlation between iMOMP and recovery following MOMP, we employed a single-cell clonogenic survival assay. For this purpose we employed HeLa cells with enforced expression of GAPDH, as described elsewhere (Collell, et al., 2007), and expressing Smac-GFP to visualize MOMP. Cells were cultured at one cell per well, treated with STS in the presence of Q-VD-OPh, and scored the following day as displaying complete or incomplete

MOMP. Wells were assessed 2 weeks later for clonogenic outgrowth (Figure 4A). We observed that cells displaying iMOMP were statistically more likely to display clonogenic recovery than those displaying complete MOMP ($p < 0.001$), thereby demonstrating a direct correlation between incomplete MOMP and survival under conditions of MOMP.

To examine this further, we employed another approach. Because Smac-GFP is degraded upon mitochondrial release, we reasoned that under conditions of CICD, cells that had undergone complete MOMP and those that had undergone iMOMP may be separated based on differential GFP fluorescence intensity (Figure 4B). HeLa cells expressing GAPDH and Smac-GFP were treated with different doses of STS in the presence of Q-VD-OPh. Flow cytometry analysis demonstrated a decrease in Smac-GFP fluorescence after STS plus Q-VD-OPh treatment (Figure 4C). Accordingly, we sorted cells into relatively low and high Smac-GFP fluorescent populations, and examined them for iMOMP by fluorescence microscopy (Figure S4A). The percentage of cells displaying iMOMP was enriched in the higher Smac-GFP fluorescence population relative to the low fluorescence population (approximately 50% versus 10%) and was independent of STS concentration (Figure 4D). Because this provided us with a means of enriching for cells displaying iMOMP, we investigated if there was a correlation between iMOMP and recovery from CICD. Following STS plus Q-VD-OPh treatment and cell sorting, equal numbers of cells from high and low Smac-GFP fluorescent populations were assessed for clonogenic outgrowth (Figure 4E). As a control for efficient induction of MOMP, HeLa cells expressing GAPDH and Smac-GFP were also examined for clonogenic outgrowth following STS treatment in the absence of caspase inhibitors, and no survival was observed (Figure 4E). Importantly, iMOMP correlated with cellular protection from conditions of CICD, because there was a marked increase in clonogenic recovery of cells from the high Smac-GFP fluorescent population relative to cells from the low fluorescence population following STS plus Q-VD-OPh treatment (Figure 4E). This protection was not observed in the absence of caspase inhibition, and was therefore not due to increased numbers of cells that had failed to engage the apoptotic pathway.

Although the percentage of cells displaying iMOMP was independent of the dose of STS, higher doses of the agent resulted in poorer clonogenic growth. We suspected that this could be due to cell damage by the STS treatment, independent of MOMP. To address this, we used HeLa cells expressing Bcl-xL and examined MOMP (by cytochrome *c* immunostaining) and clonogenic survival following treatment with STS. Of note, whereas Bcl-xL inhibited MOMP at all doses of STS, clonogenic growth was observed only at the lower doses (Figure S4B). Therefore, the decreased clonogenic survival we observed at increased doses of STS in the experiment in Figure 4E is likely representative of cell damage irrespective of apoptosis.

Bax and Bak Fail to Be Activated on Nonpermeabilized Mitochondria

We next investigated the underlying mechanism(s) that resulted in certain mitochondria being refractory to MOMP. Pro- and antiapoptotic members of the Bcl-2 family regulate the integrity of the mitochondrial outer membrane; during apoptosis activation of the proapoptotic proteins Bax and/or Bak induces MOMP (Chipuk and Green, 2008). We monitored Bax translocation because the proapoptotic activity of Bax is inextricably linked to its translocation from the cytoplasm to mitochondria. HeLa cells expressing GFP-Bax and Omi-mCherry were treated with UV or ActD in the presence of Q-VD-OPh and examined by live-cell microscopy. Mitochondrial release of Omi-mCherry was accompanied by mitochondrial translocation of GFP-Bax (Figure 5A; Movie S5). Examination of cells displaying iMOMP revealed that intact mitochondria failed to accumulate GFP-Bax, suggesting that the failure of certain mitochondria to undergo MOMP is associated with an absence of Bax activation at these mitochondria.

To rule out any confounding effects of endogenous Bax or Bak, we carried out similar imaging experiments in Bax/Bak double knockout MEF (DKO MEF) expressing GFP-Bax and Omi-mCherry. Expression of GFP-Bax in DKO MEF fully restored their apoptotic sensitivity (data not shown). DKO MEF expressing GFP-Bax and Omi-mCherry were treated with either UV or ActD in the presence of Q-VD-OPh and imaged the following day. As we previously observed, GFP-Bax failed to translocate to intact mitochondria in cells displaying iMOMP (Figure 5B). A previous study has shown that Bax and Bak form clusters adjacent to mitochondria following their activation (Nechushtan et al., 2001). However, following MOMP we could clearly detect the presence of intact mitochondria that had no GFP-Bax in close proximity, indicating a failure of Bax activation on these mitochondria.

We employed a similar approach to address the role of Bak during incomplete MOMP by expressing GFP-Bak and Omi-mCherry in DKO MEF. Expression of GFP-Bak in these cells fully restored their apoptotic sensitivity (data not shown). DKO cells expressing GFP-Bak and Omi-mCherry were treated with either UV or ActD in the presence of Q-VD-OPh and imaged the following day (Figure 5C). As expected, GFP-Bak displayed constitutive mitochondrial localization. In cells that displayed iMOMP, GFP-Bak was nevertheless present on mitochondria that remained intact, suggesting that Bak, similar to Bax, fails to be activated on these mitochondria.

Antiapoptotic Bcl-2 Proteins Promote iMOMP

The failure to activate Bax/Bak proteins on some mitochondria might allow them to evade MOMP. We hypothesized that this failure to activate Bax and Bak may be due to antiapoptotic Bcl-2 activity. To address this, we investigated Bcl-2 levels on intact mitochondria following MOMP. HeLa cells expressing Omi-mCherry and GFP-Bcl-2 were treated with UV or ActD in the presence of Q-VD-OPh and imaged the following day (Figure 6A; Figure S5). In cells displaying iMOMP, increased levels of GFP-Bcl-2 were observed on intact versus permeabilized mitochondria, suggesting that antiapoptotic Bcl-2 proteins are responsible for protecting the intact mitochondria.

To further test this hypothesis, we employed cell fusion experiments between HeLa cells expressing Smac 1-60 mCherry and Cerulean and HeLa cells overexpressing Bcl-2 and Smac-YFP. Fused cells were identified by the presence of cytosolic Cerulean protein in Smac-YFP cells. Cells were treated with UV in the presence of Q-VD-OPh and imaged (Figure 6B). In fused cells, mitochondria expressing Smac YFP and Bcl-2 failed to undergo

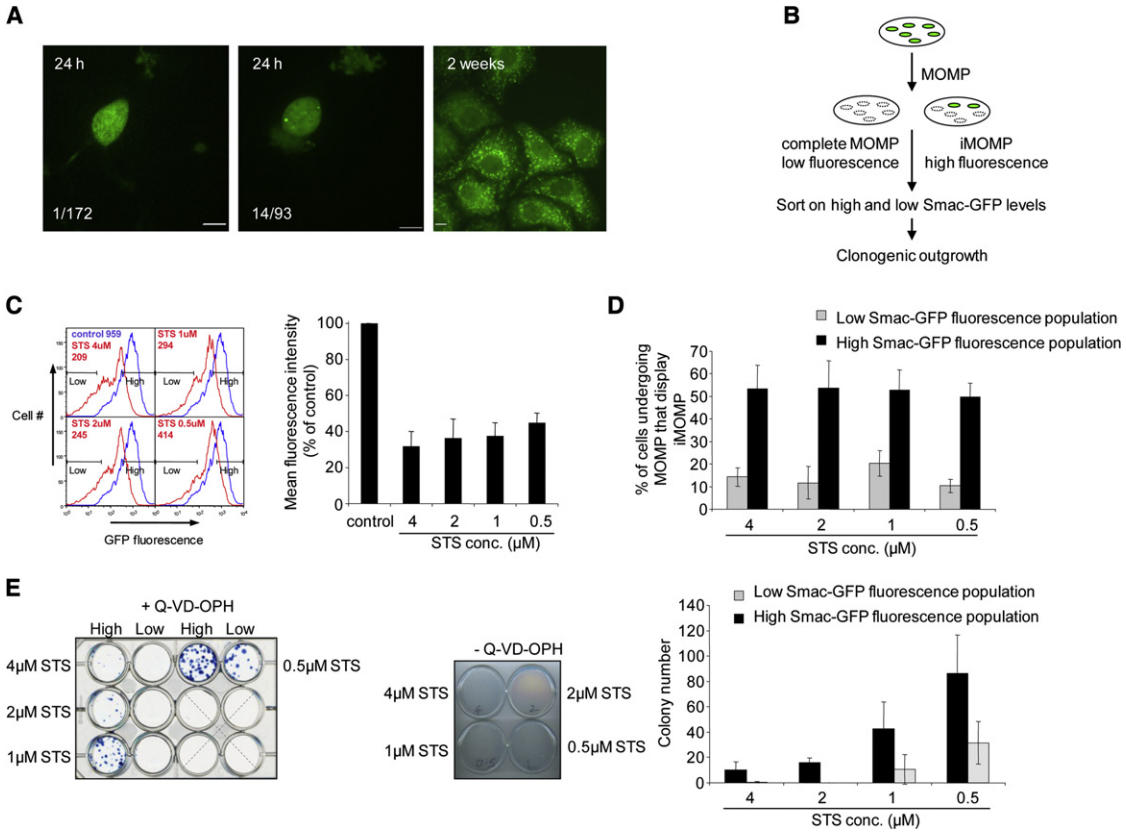

Figure 4. Incomplete MOMP Correlates with Cellular Recovery from CICD

(A) Left/center: Representative confocal micrographs from single-cell cultures showing complete (left) and incomplete (center) MOMP in HeLa cells expressing GAPDH and Smac-GFP following 16 hr treatment with STS (1 μM) plus Q-VD-OPh (20 μM). Right: Widefield micrograph of a proliferating colony 14 days later. Inset numbers refer to the number of proliferating colonies that arose/the number of cells analyzed that display either complete or incomplete MOMP. The difference between groups was assessed by chi-square analysis ($p < 0.001$).

(B) Schematic experimental outline. HeLa cells expressing Smac-GFP following STS treatment leading to complete MOMP will display less relative fluorescence than those displaying iMOMP. These cell populations are sorted by flow cytometry and assessed for their ability to exhibit clonogenic survival.

(C) HeLa cells expressing Smac-GFP were treated for 16 hr with STS (0.5-4 μM) plus Q-VD-OPh (20 μM) and analyzed by flow cytometry for GFP fluorescence intensity (inset, mean fluorescence intensity [MFI]). Gates denote populations covering 20% lowest and highest Smac-GFP fluorescent populations that were sorted. Quantification of Smac-GFP MFI of STS plus Q-VD-OPh-treated cells from three independent experiments expressed as percentage relative to control untreated cells. Error bars represent SD.

(D) HeLa cells expressing Smac-GFP were treated for 16 hr with STS (0.5-4 μM) plus Q-VD-OPh (20 μM) and sorted into the 20% highest and lowest GFP-expressing cells and analyzed by microscopy for iMOMP. Number of cells displaying iMOMP as a percentage of cells displaying MOMP is shown, a minimum 100 cells per condition were counted. Results are from three independent experiments ± SD.

(E) HeLa cells expressing GAPDH and Smac-GFP were treated for 16 hr with STS (0.5 μM-4 μM) plus Q-VD-OPh (20 μM) and sorted into 20% highest and lowest GFP-expressing populations. Then 2×10^5 cells from each population were plated down in the presence of Q-VD-OPh (20 μM) and examined for clonogenic outgrowth. As a control, 1×10^6 cells were treated with STS (0.5-4 μM) for 16 hr and examined for clonogenic outgrowth (middle panel). Colony number from three independent experiments; error bars represent SD. Scale bars represent 10 μm. See also Figure S4.

MOMP whereas Smac 1-60-mCherry was released from the control mitochondria. This result indicates that increased levels of antiapoptotic Bcl-2 proteins on certain mitochondria can protect these mitochondria from MOMP.

We then examined the effects of ABT-737, a compound that has been developed as a BH3 mimetic that inhibits the antiapoptotic function of Bcl-2, Bcl-xL, and Bcl-w (Oltersdorf et al., 2005). We treated HeLa cells expressing Smac-GFP with ActD in the presence of Q-VD-OPh. Exposure of cells to ABT-737 in the absence of ActD did not induce MOMP or affect cell viability (Figure 6E and data not shown). The following day, after cells had undergone MOMP, ABT-737 or its inactive enantiomer was added and cells displaying iMOMP were imaged by live-cell microscopy (Figure 6C; Movies S6 and S7). Strikingly, following treatment with ABT-737, intact mitochondria in these cells underwent complete MOMP, whereas intact mitochondria persisted in cells treated with enantiomer. Alternatively, cells were treated overnight with STS plus Q-VD-OPh or UV plus Q-VD-OPh in the presence of ABT-737 or enantiomer and assessed for iMOMP the following day. Coincubation with ABT-737 significantly reduced the number of cells displaying iMOMP either before or after UV or STS treatment relative to those that were treated with enantiomer (Figure 6D). These data show that, following different apoptotic stimuli, iMOMP

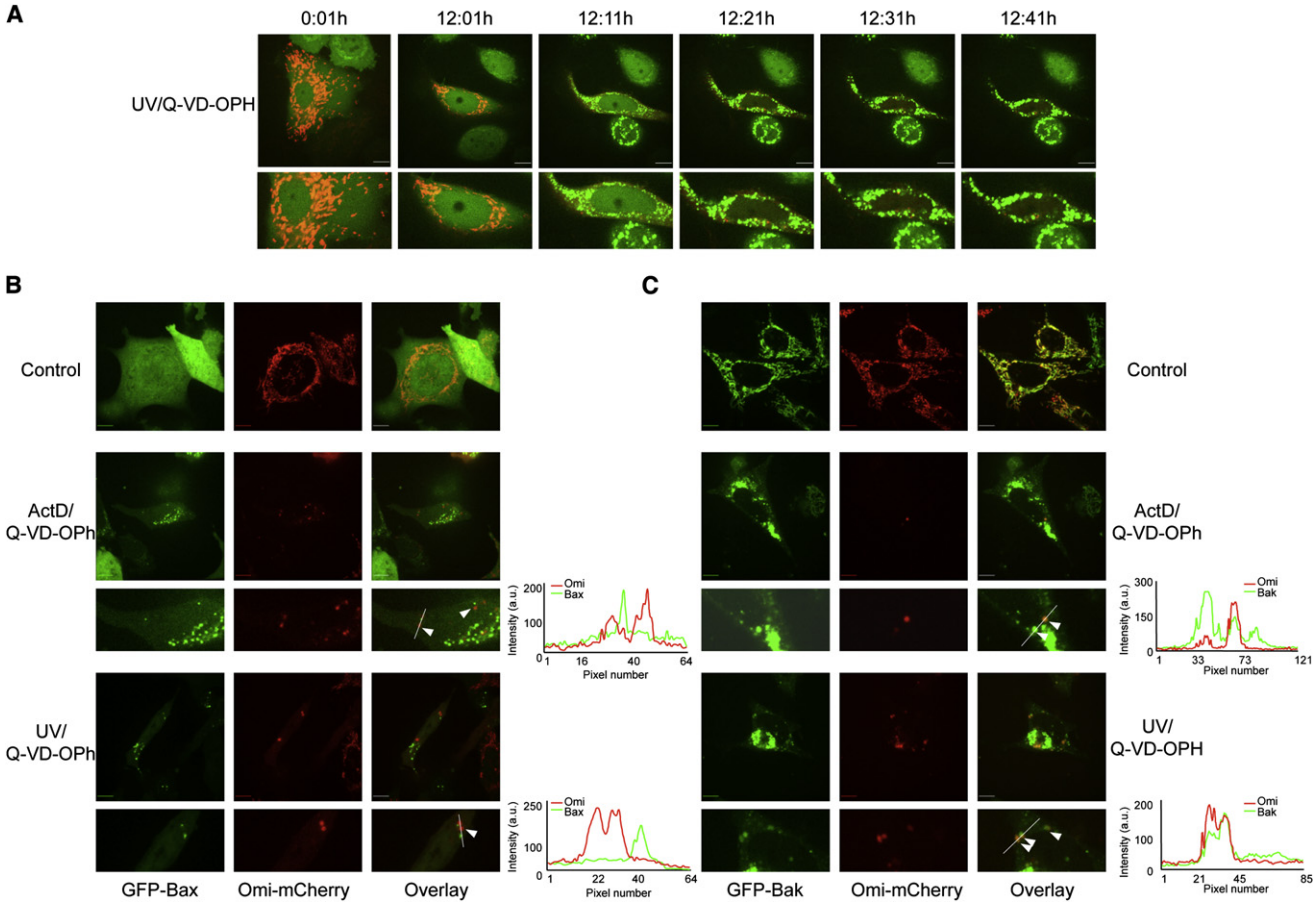

Figure 5. Bax and Bak Fail to Be Activated on Nonpermeabilized Mitochondria

(A) HeLa cells expressing GFP-Bax and Omi-mCherry were treated with UV (18 mJ/cm^2) plus Q-VD-OPh (20 μM) and imaged every 10 min by live-cell microscopy. Representative confocal micrographs covering the onset and duration of MOMP are shown. The time of each frame relative to the start of image acquisition is shown.

(B) Bax/Bak DKO MEFs expressing GFP-Bax and Omi-mCherry were untreated or treated with UV (18 mJ/cm^2) or ActD (1 μM) plus Q-VD-OPh (20 μM). Representative confocal micrographs are shown. Arrows denote intact mitochondria that fail to have GFP-Bax in close proximity.

(C) Bax/Bak DKO MEFs expressing GFP-Bak and Omi-mCherry were untreated or treated with UV (18mJ/cm^2) or ActD (1 μM) plus Q-VD-OPh (20 μM). Representative confocal micrographs are shown. Arrows denote intact mitochondria. Line scans indicate colocalization of Omi-mCherry and GFP-Bak and correlate to the line drawn in the images. Scale bars represent 10 μm.

can be converted to complete MOMP by antagonizing antiapoptotic Bcl-2 function, supporting a model that antiapoptotic Bcl-2 protein function enables iMOMP.

Given the effect of ABT-737 on incidence of iMOMP, we next examined the effect of ABT-737 treatment on the ability of cells to recover from conditions of CICD. HeLa cells expressing GAPDH were treated with STS in the presence or absence of Q-VD-OPh. Cells were treated with ABT-737 or enantiomer either prior to or after treatment with STS and assessed for clonogenic survival. Incubation of cells with ABT-737 alone had no effect on cell viability (Figure 6E). Caspase inhibition promoted clonogenic recovery, indicating protection from CICD. However, incubation of cells with ABT-737 either prior to or after STS plus Q-VD-OPh treatment effectively blocked clonogenic survival, further supporting a key role for intact mitochondria in the ability of cells to be protected from conditions of CICD and recover following MOMP.

DISCUSSION

Mitochondrial outer membrane permeabilization initiates apoptosis by activating executioner caspases; however, even when caspase activation is blocked, cells nonetheless die following MOMP, an observation believed to be explained by the requirement for intact mitochondria to sustain cellular metabolism. This view is supported by data from our own lab (Collell et al., 2007) showing that enforced expression of the metabolic enzyme GAPDH can permit recovery following MOMP. However, previous studies failed to address how cells recover and repopulate their mitochondria following MOMP. Our results show that during apoptosis, MOMP can be incomplete, leaving some mitochondria intact. These data demonstrate a correlation between iMOMP and clonogenic survival following MOMP, and show that this survival can be blocked if iMOMP is disrupted. Based on these results, we propose that iMOMP provides a critical

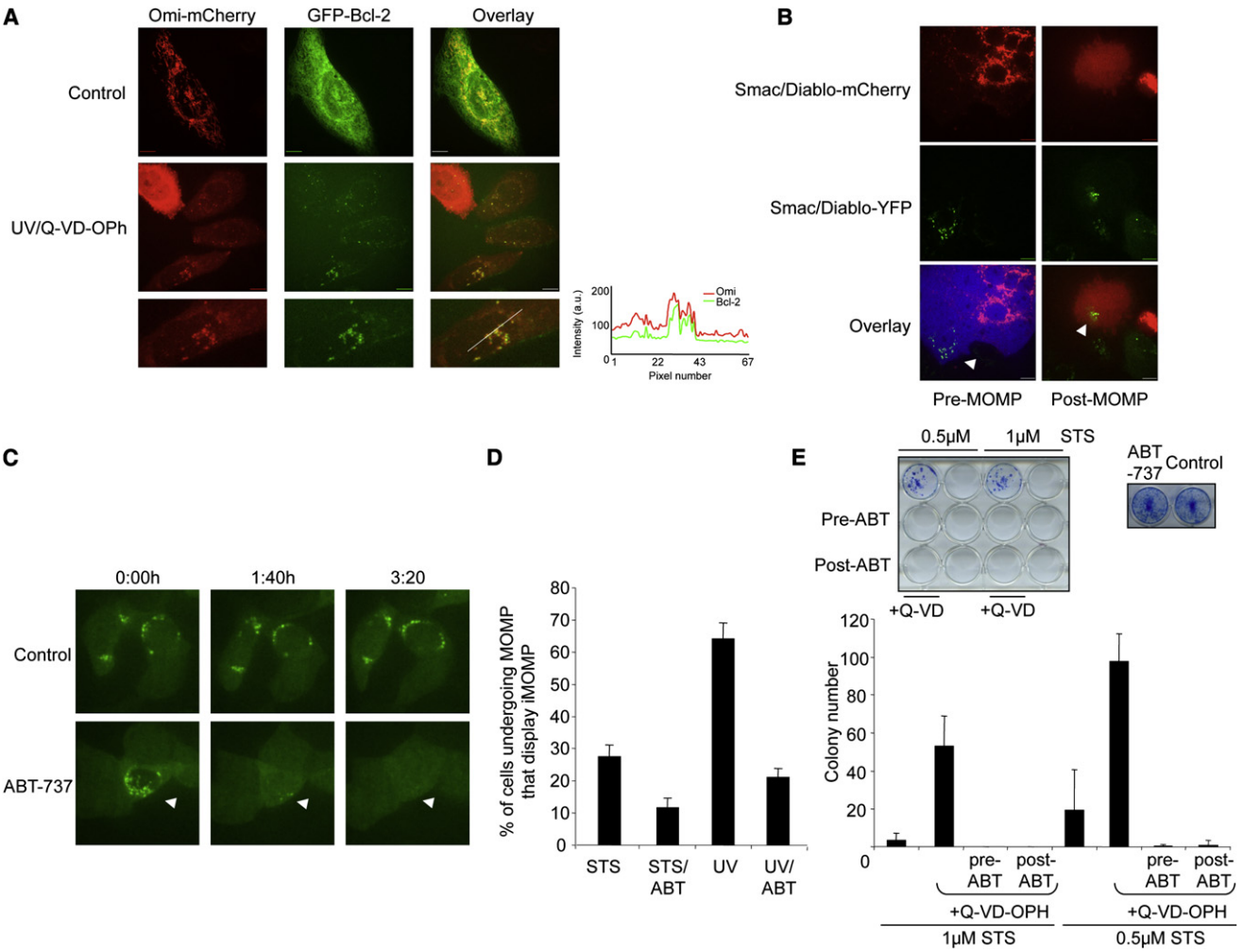

Figure 6. Antiapoptotic Bcl-2 Proteins Promote iMOMP

(A) HeLa cells expressing GFP-Bcl-2 and Omi-mCherry were untreated or treated with UV (18 mJ/cm^2) plus Q-VD-OPh (20 μM). Representative confocal micrographs are shown. Line scans indicate co-localization of Omi-mCherry and GFP-Bcl-2 and correlate to the line drawn in the images.

(B) HeLa cells expressing Smac 1-60-mCherry/Cerulean and HeLa cells expressing Bcl-2 and Smac-YFP were fused, treated overnight with UV (18mJ/cm^2) plus Q-VD-OPh (20 μM) and imaged by live-cell microscopy. Representative confocal micrographs pre- and post-MOMP are shown. Arrow denotes intact mitochondria.

(C) MCF-7 cells expressing Smac-GFP were treated overnight with ActD (1 μM) plus Q-VD-OPh (20 μM) then treated the following day with enantiomer or ABT-737 (both 10 μM) and imaged every 10 min by live-cell confocal microscopy. The time of each frame relative to the start of image acquisition is shown and arrows denote cells undergoing iMOMP.

(D) HeLa cells expressing Smac-GFP were treated for 16 hr with ABT-737 or enantiomer (both 1 μM) then treated for 16 hr with STS (1 μM) plus Q-VD-OPh (20 μM) or (18mJ/cm^2) plus Q-VD-OPh. The percentage of cells displaying iMOMP as a percentage of cells displaying MOMP is shown from three independent experiments (minimum 100 cells counted). Error bars represent SD.

(E) HeLa cells expressing GAPDH and Smac-GFP were treated with STS (0.5 or 1 μM) ± Q-VD-OPh (20 μM) for 16 hr. Where indicated, prior to or after STS treatment, ABT-737 or enantiomer was added (1 μM) for 16 hr. As indicated, Q-VD-OPh was replenished for a further 3 days and cells were assessed for clonogenic outgrowth. As a control, HeLa cells expressing GAPDH and Smac-GFP were cultured ± ABT-737 (1 μM) for 3 days. Colony number from three independent experiments ± SD is shown. Scale bars represent 10 μm. See also Figure S5.

cohort of healthy mitochondria that permits cellular recovery from MOMP (Figure 7).

Our discovery that MOMP can be incomplete contrasts with one of our previous studies that concluded MOMP is an all-or-nothing event based on imaging cell cells expressing cytochrome *c*-GFP (Goldstein et al., 2000). By making use of Smac and Omi fluorescent fusion proteins, we suspect that our ability to visualize iMOMP has been greatly enhanced for two reasons. Unlike cytochrome *c*, Smac and Omi fluorescent fusion proteins undergo cytoplasmic degradation following MOMP, thereby facilitating the detection of intact mitochondria that remain brighter (Figure 1A). Second, unlike cytochrome *c*, Smac and Omi fluorescent fusion proteins displayed minimal mislocalization in healthy cells, further enhancing the resolution with which MOMP could be tracked. However we also found, using imaging techniques that are improved from those earlier (Goldstein et al.,

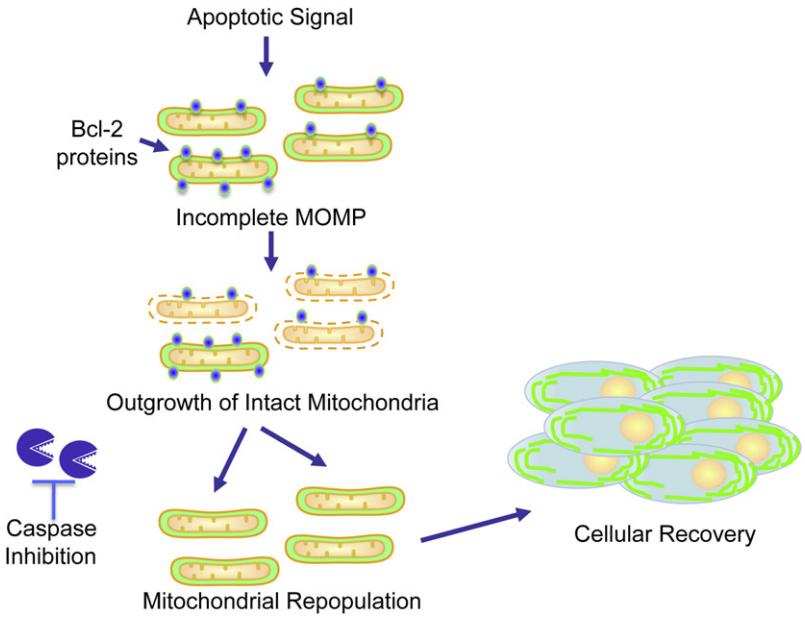

Figure 7. Model of Mitochondrial Repopulation Required for Cellular Recovery from MOMP

Following an apoptotic stimulus, the majority of mitochondria within a cell undergo MOMP. However, MOMP can be incomplete; some mitochondria remain intact due to increased levels of antiapoptotic Bcl-2 proteins on their outer membranes. Over time, these intact mitochondria repopulate the cell, enabling cell survival and proliferation under conditions where caspase function is inhibited.

2000), that similar to our results with Smac and Omi, the release of cytochrome *c*-GFP can also be observed to be incomplete (Figure S1). That these mitochondria are indeed intact is evidenced by the presence of all IMS proteins tested, and by the persistence of $\Delta\Psi$m (Figure 3A).

How do mitochondria selectively evade MOMP? Our data support a model whereby some mitochondria within a cell have increased antiapoptotic Bcl-2 activity and are therefore refractory to MOMP. This is based on several findings: Bax failed to accumulate on mitochondria and Bak does not cluster adjacent to mitochondria that have not undergone MOMP (Figure 5), increased levels of Bcl-2 can protect specific mitochondria from MOMP (Figures 6A and 6B), and the Bcl-2 antagonist ABT-737 induces the permeabilization of intact mitochondria in cells displaying iMOMP (Figures 6C and 6D). Interestingly, the selective failure of Bax to accumulate at nonpermeabilized mitochondria suggests that the critical steps of Bax activation (e.g., conformational changes leading to oligomerization) likely occur at the target mitochondrial membrane rather than in the cytoplasm as supported by a recent study showing that Bax activation requires a membrane environment (Lovell et al., 2008). Although ABT-737 effectively promoted complete MOMP in most cells, some cells were refractory to its addition (not shown). This may be attributable to the inability of ABT-737 to inhibit all antiapoptotic Bcl-2 family proteins such as Mcl-1 (Oltersdorf et al., 2005) or, perhaps more interestingly, there may be alternative mechanisms that allow mitochondria to selectively evade MOMP.

Mitochondrial fragmentation accompanies but is not required for MOMP (Estaquier and Arnoult, 2007; Parone et al., 2006). Our results demonstrate that mitochondrial dynamics play a key role in iMOMP: inhibition of mitochondrial fission reduced the incidence of iMOMP whereas promoting fission had the opposite effect (Figure 3E). Presumably this outcome relates to the interconnectivity between the IMS of different mitochondria; a mitochondrion that is resistant to MOMP when in isolation would be expected to release its IMS contents if it were fused to a permeabilized mitochondria. Because MOMP and mitochondrial fragmentation occur almost simultaneously, it is currently unclear if intact mitochondria are separated prior to MOMP or undergo fission at the time of MOMP.

The correlation between iMOMP and clonogenic survival under conditions of CICD coupled with the ability to block protection by inhibiting iMOMP supports a functional consequence of iMOMP (Figures 4A, 4E, and 6E). Recovery from MOMP typically takes several days (Colell et al., 2007). Long-term imaging revealed that intact mitochondria persist over time and that mitochondrial repopulation occurs in some cells. Intact mitochondria could be observed to apparently undergo fission, even at early periods post-MOMP. We propose that iMOMP provides a source of "seed" mitochondria that are required to regenerate the mitochondrial population prior to full cell recovery. Unfortunately, it remains technically challenging to permanently mark these mitochondria and follow them over time. Therefore, another possibility is that functional, nonpermeabilized mitochondria are required only temporarily to compensate for the functional decline that is observed in permeabilized mitochondria over time (Colell et al., 2007). However, this model would require an alternative means of generating healthy mitochondria by resealing of the mitochondrial outer membrane following MOMP. We have not observed such an appearance of intact mitochondria in cells displaying complete MOMP, but such a mechanism cannot be formally excluded.

Previously, we have shown that recovery post-MOMP involves autophagic removal of mitochondria, also termed mitophagy, prior to cell recovery (Colell et al., 2007). In the present study we found that intact mitochondria persist in cells at least over a 3 day period, suggesting that they are spared from removal (Figure S3). In the context of mitophagy, cells displaying iMOMP may serve as a useful means to study the mechanisms by which a cell can discriminate between damaged and healthy mitochondria.

Perhaps of direct clinical relevance, we show that ABT-737 can effectively inhibit iMOMP and block cellular protection from CICD (Figure 6). This result suggests that the chemotherapeutic potency of ABT-737 may also be linked to its ability to block tumor cell resistance to conditions of CICD by inhibiting iMOMP. Alternatively, in scenarios where caspase inhibitors might be used as cytoprotective agents then one might predict that promotion of iMOMP would facilitate cell survival leading to greater therapeutic efficacy.

EXPERIMENTAL PROCEDURES

Cell Treatments

To induce apoptosis, cells were treated with the indicated concentrations of staurosporine (Sigma), human TNF (Peprotech), actinomycin D (Sigma), or UV irradiated using a Stratagene UV crosslinker. Where indicated, the pan-caspase inhibitor Q-VD-OPh was added to a final concentration of 20 μM (EMD Biosciences). ABT-737 and enantiomer were obtained from Abbot Laboratories. Where indicated, cells were incubated with 25 μM FCCP (Sigma) for 1 hr prior to washing and readdition of culture medium.

Microscopy

Cells were plated on dishes containing fibronectin-coated coverslips (Mattek) 24 hr prior to treatment and imaged using a spinning disk confocal microscope (Zeiss). For time-lapse experiments, media on the cells was supplemented with HEPES (20 mM) and 2-mercaptoethanol (55 μM) prior to imaging.

Clonogenic Survival Assays

Following overnight treatment, HeLa cells expressing Smac GFP and GAPDH were sorted into the lowest and highest 20% fluorescent populations, and 2×10^5 cells from both populations were washed and plated in a 12-well plate. For the ABT-737 clonogenic assays, 2.5×10^3 cells/per well were plated down on a 12-well plate 2 days prior to treatment. The following day, cells were treated with ABT-737 or enantiomer overnight (both at 1 μM), then treated with ABT-737 or enantiomer plus STS ± Q-VD-OPh for 8 hr. Where noted, ABT-737 or enantiomer was added at 1 μM for 16 hr posttreatment. The following, day cells were washed and incubated with new media ± Q-VD-OPh. Where added, Q-VD-OPh was refreshed for the next 2 days. Following clonogenic outgrowth, colonies were visualized by staining with methylene blue 0.1% w/v in methanol/water 50% v/v for 20 min.

SUPPLEMENTAL INFORMATION

Supplemental Information includes five figures, Supplemental Experimental Procedures, and seven movies and can be found with this article online at doi:10.1016/j.devcel.2010.03.014.

ACKNOWLEDGMENTS

We thank Roger Tsien, Damien Arnoult, and David Piston for providing plasmids, and Abbott Laboratories for providing ABT-737. We also thank Richard Cross, Greig Lennon, and the St. Jude Flow Cytometry facility for cell sorting; Kiri Ness for statistical analysis; and Andrew Oberst, Christopher Dillon, Tudor Moldoveanu, and Jacqueline Tait-Mulder (St. Jude Children's Research Hospital) for critical reading of the manuscript. This work was supported by NIH AI40646 and the American Lebanese Syrian Associated Charities.

Received: July 23, 2009
Revised: December 14, 2009
Accepted: March 1, 2010
Published: May 17, 2010

REFERENCES

Amarante-Mendes, G.P., Finucane, D.M., Martin, S.J., Cotter, T.G., Salvesen, G.S., and Green, D.R. (1998). Anti-apoptotic oncogenes prevent caspase-dependent and independent commitment for cell death. Cell Death Differ. *5*, 298–306.

Cereghetti, G.M., Stangherlin, A., Martins de Brito, O., Chang, C.R., Blackstone, C., Bernardi, P., and Scorrano, L. (2008). Dephosphorylation by calcineurin regulates translocation of Drp1 to mitochondria. Proc. Natl. Acad. Sci. USA *105*, 15803–15808.

Chipuk, J.E., and Green, D.R. (2008). How do BCL-2 proteins induce mitochondrial outer membrane permeabilization? Trends Cell Biol. *18*, 157–164.

Colell, A., Ricci, J.E., Tait, S., Milasta, S., Maurer, U., Bouchier-Hayes, L., Fitzgerald, P., Guio-Carrion, A., Waterhouse, N.J., Li, C.W., et al. (2007). GAPDH and autophagy preserve survival after apoptotic cytochrome c release in the absence of caspase activation. Cell *129*, 983–997.

Deshmukh, M., Kuida, K., and Johnson, E.M., Jr. (2000). Caspase inhibition extends the commitment to neuronal death beyond cytochrome c release to the point of mitochondrial depolarization. J. Cell Biol. *150*, 131–143.

Devarajan, E., Sahin, A.A., Chen, J.S., Krishnamurthy, R.R., Aggarwal, N., Brun, A.M., Sapino, A., Zhang, F., Sharma, D., Yang, X.H., et al. (2002). Down-regulation of caspase 3 in breast cancer: a possible mechanism for chemoresistance. Oncogene *21*, 8843–8851.

Estaquier, J., and Arnoult, D. (2007). Inhibiting Drp1-mediated mitochondrial fission selectively prevents the release of cytochrome c during apoptosis. Cell Death Differ. *14*, 1086–1094.

Ferreira, C.G., van der Valk, P., Span, S.W., Ludwig, I., Smit, E.F., Kruyt, F.A., Pinedo, H.M., van Tinteren, H., and Giaccone, G. (2001). Expression of X-linked inhibitor of apoptosis as a novel prognostic marker in radically resected non-small cell lung cancer patients. Clin. Cancer Res. *7*, 2468–2474.

Goldstein, J.C., Waterhouse, N.J., Juin, P., Evan, G.I., and Green, D.R. (2000). The coordinate release of cytochrome c during apoptosis is rapid, complete and kinetically invariant. Nat. Cell Biol. *2*, 156–162.

Goldstein, J.C., Munoz-Pinedo, C., Ricci, J.E., Adams, S.R., Kelekar, A., Schuler, M., Tsien, R.Y., and Green, D.R. (2005). Cytochrome c is released in a single step during apoptosis. Cell Death Differ. *12*, 453–462.

Haraguchi, M., Torii, S., Matsuzawa, S., Xie, Z., Kitada, S., Krajewski, S., Yoshida, H., Mak, T.W., and Reed, J.C. (2000). Apoptotic protease activating factor 1 (Apaf-1)-independent cell death suppression by Bcl-2. J. Exp. Med. *191*, 1709–1720.

Krajewska, M., Krajewski, S., Banares, S., Huang, X., Turner, B., Bubendorf, L., Kallioniemi, O.P., Shabaik, A., Vitiello, A., Peehl, D., et al. (2003). Elevated expression of inhibitor of apoptosis proteins in prostate cancer. Clin. Cancer Res. *9*, 4914–4925.

Lakhani, S.A., Masud, A., Kuida, K., Porter, G.A., Jr., Booth, C.J., Mehal, W.Z., Inayat, I., and Flavell, R.A. (2006). Caspases 3 and 7: key mediators of mitochondrial events of apoptosis. Science *311*, 847–851.

Li, L.Y., Luo, X., and Wang, X. (2001). Endonuclease G is an apoptotic DNase when released from mitochondria. Nature *412*, 95–99.

Lovell, J.F., Billen, L.P., Bindner, S., Shamas-Din, A., Fradin, C., Leber, B., and Andrews, D.W. (2008). Membrane binding by tBid initiates an ordered series of events culminating in membrane permeabilization by Bax. Cell *135*, 1074–1084.

Lum, J.J., Bauer, D.E., Kong, M., Harris, M.H., Li, C., Lindsten, T., and Thompson, C.B. (2005). Growth factor regulation of autophagy and cell survival in the absence of apoptosis. Cell *120*, 237–248.

MacFarlane, M., Merrison, W., Bratton, S.B., and Cohen, G.M. (2002). Proteasome-mediated degradation of Smac during apoptosis: XIAP promotes Smac ubiquitination in vitro. J. Biol. Chem. *277*, 36611–36616.

Martinou, I., Desagher, S., Eskes, R., Antonsson, B., Andre, E., Fakan, S., and Martinou, J.C. (1999). The release of cytochrome c from mitochondria during apoptosis of NGF-deprived sympathetic neurons is a reversible event. J. Cell Biol. *144*, 883–889.

McCarthy, N.J., Whyte, M.K., Gilbert, C.S., and Evan, G.I. (1997). Inhibition of Ced-3/ICE-related proteases does not prevent cell death induced by oncogenes, DNA damage, or the Bcl-2 homologue Bak. J. Cell Biol. *136*, 215–227.

Munoz-Pinedo, C., Guio-Carrion, A., Goldstein, J.C., Fitzgerald, P., Newmeyer, D.D., and Green, D.R. (2006). Different mitochondrial intermembrane space proteins are released during apoptosis in a manner that is coordinately initiated but can vary in duration. Proc. Natl. Acad. Sci. USA *103*, 11573–11578.

Nechushtan, A., Smith, C.L., Lamensdorf, I., Yoon, S.H., and Youle, R.J. (2001). Bax and Bak coalesce into novel mitochondria-associated clusters during apoptosis. J. Cell Biol. *153*, 1265–1276.

Oltersdorf, T., Elmore, S.W., Shoemaker, A.R., Armstrong, R.C., Augeri, D.J., Belli, B.A., Bruncko, M., Deckwerth, T.L., Dinges, J., Hajduk, P.J., et al. (2005). An inhibitor of Bcl-2 family proteins induces regression of solid tumours. Nature *435*, 677–681.

Parone, P.A., James, D.I., Da Cruz, S., Mattenberger, Y., Donze, O., Barja, F., and Martinou, J.C. (2006). Inhibiting the mitochondrial fission machinery does not prevent Bax/Bak-dependent apoptosis. Mol. Cell. Biol. *26*, 7397–7408.

Schmitt, C.A., Fridman, J.S., Yang, M., Baranov, E., Hoffman, R.M., and Lowe, S.W. (2002). Dissecting p53 tumor suppressor functions in vivo. Cancer Cell *1*, 289–298.

Soengas, M.S., Capodieci, P., Polsky, D., Mora, J., Esteller, M., Opitz-Araya, X., McCombie, R., Herman, J.G., Gerald, W.L., Lazebnik, Y.A., et al. (2001). Inactivation of the apoptosis effector Apaf-1 in malignant melanoma. Nature *409*, 207–211.

Sun, X.M., Butterworth, M., MacFarlane, M., Dubiel, W., Ciechanover, A., and Cohen, G.M. (2004). Caspase activation inhibits proteasome function during apoptosis. Mol. Cell *14*, 81–93.

Susin, S.A., Lorenzo, H.K., Zamzami, N., Marzo, I., Snow, B.E., Brothers, G.M., Mangion, J., Jacotot, E., Costantini, P., Loeffler, M., et al. (1999). Molecular characterization of mitochondrial apoptosis-inducing factor. Nature *397*, 441–446.

Suzuki, Y., Imai, Y., Nakayama, H., Takahashi, K., Takio, K., and Takahashi, R. (2001). A serine protease, HtrA2, is released from the mitochondria and interacts with XIAP, inducing cell death. Mol. Cell *8*, 613–621.

Tait, S.W., and Green, D.R. (2008). Caspase-independent cell death: leaving the set without the final cut. Oncogene *27*, 6452–6461.

Tamm, I., Kornblau, S.M., Segall, H., Krajewski, S., Welsh, K., Kitada, S., Scudiero, D.A., Tudor, G., Qui, Y.H., Monks, A., et al. (2000). Expression and prognostic significance of IAP-family genes in human cancers and myeloid leukemias. Clin. Cancer Res. *6*, 1796–1803.

Taylor, R.C., Cullen, S.P., and Martin, S.J. (2008). Apoptosis: controlled demolition at the cellular level. Nat. Rev. Mol. Cell Biol. *9*, 231–241.

Waterhouse, N.J., Goldstein, J.C., von Ahsen, O., Schuler, M., Newmeyer, D.D., and Green, D.R. (2001). Cytochrome c maintains mitochondrial transmembrane potential and ATP generation after outer mitochondrial membrane permeabilization during the apoptotic process. J. Cell Biol. *153*, 319–328.

Wolf, B.B., Schuler, M., Li, W., Eggers-Sedlet, B., Lee, W., Tailor, P., Fitzgerald, P., Mills, G.B., and Green, D.R. (2001). Defective cytochrome c-dependent caspase activation in ovarian cancer cell lines due to diminished or absent apoptotic protease activating factor-1 activity. J. Biol. Chem. *276*, 34244–34251.

Xiang, J., Chao, D.T., and Korsmeyer, S.J. (1996). BAX-induced cell death may not require interleukin 1 beta-converting enzyme-like proteases. Proc. Natl. Acad. Sci. USA *93*, 14559–14563.